

Heat capacity of synthetic hydrous Mg-cordierite at low temperatures: Thermodynamic properties and the behavior of the H₂O molecule in selected hydrous micro and nanoporous silicates

IGOR E. PAUKOV,¹ YULIA A. KOVALEVSKAYA,¹ NOURI-SAID RAHMOUN,² AND CHARLES A. GEIGER^{2,*}

¹Institute of Inorganic Chemistry, Lavrentiev prosp. 3, Novosibirsk 630090, Russia

²Institut für Geowissenschaften, Abteilung Mineralogie, Universität Kiel, Olshausenstrasse 40, D-24098 Kiel, Germany

ABSTRACT

The heat capacity, C_p , of a synthetic hydrous cordierite of composition $\text{Mg}_{1.97}\text{Al}_{3.94}\text{Si}_{5.06}\text{O}_{18} \cdot 0.625\text{H}_2\text{O}$ was measured for the first time using precise adiabatic calorimetry in the temperature range from 6 to 300 K. Hydrous Mg-cordierite was obtained by hydrothermal treatment of anhydrous Mg-cordierite (Paukov et al. 2006) at 4 kbar and 600 °C for 24 hours. The synthetic product was characterized using X-ray diffraction and powder IR spectroscopy. Rietveld refinement gives $a = 17.060(2)$ Å, $b = 9.721(1)$ Å, and $c = 9.338(1)$ Å with $V = 1548.7(3)$ Å³ and $\Delta = 0.25$, and the IR spectrum shows only the presence of Class I-Type I H₂O in the channel cavities. Small C_p anomalies were observed at 272.98 ± 0.03 K and 239.43 ± 0.13 K, which are thought to be related to very small amounts of H₂O occurring in tiny fluid inclusions and to surface H₂O, respectively. From the heat-capacity data on hydrous Mg-cordierite, various thermodynamic functions were calculated and are presented in table form. The calculated partial molar entropy for one mole of H₂O in hydrous Mg-cordierite at 298.15 K and 1 bar is 80.5 J/(mol·K). The partial molar volume for H₂O in hydrous Mg-cordierite at 298 K and 1 bar is zero. The C_p results, together with published heat-capacity data on three different zeolites, permit a comparison and analysis of their heat-capacity behavior. The heat-capacity behavior of H₂O molecules in zeolites is more similar to that of ice at $T < 300$ K and not to gaseous H₂O, which can be attributed to the presence of hydrogen-bonded H₂O molecules. In contrast, the heat-capacity behavior for the “quasi-free” H₂O molecule in cordierite is more similar to that of a free H₂O molecule in the gaseous state between approximately 100 and 300 K. At $T < 100$ K, the energies of low-energy modes, especially external H₂O translations, determine heat-capacity behavior. Model heat capacities for H₂O in cordierite were calculated using the Einstein model and using as input data the results from inelastic neutron-scattering measurements on hydrous Mg-cordierite (Winkler and Hennion 1994). Reasonable agreement between experiment and calculations can be achieved using three H₂O translational modes, one of which is hypothetical, and two librational H₂O modes. The experimental spectra do not appear to show all six external H₂O modes and further vibrational spectroscopic study is required to determine their energies. At $T > 300$ K, the heat capacity for H₂O is the smallest in steam with values increasing in hydrous beryl and cordierite, to H₂O in various zeolites, and finally to liquid H₂O. This behavior may reflect the nature of the hydrogen bonding and the energies of internal H₂O stretching modes, which decrease in energy with increasing hydrogen-bonding strength in the various systems.

Keywords: Hydrous Mg-cordierite, heat capacity, adiabatic calorimetry, H₂O molecule, micro and nanoporous silicates

INTRODUCTION

The H₂O molecule plays a fundamental role in various geological and biomineralogical processes. Indeed, much effort is being invested, for example, in studying the nature of various fluid-geomaterial interactions and biological-geological processes. To obtain a fundamental scientific understanding of such complex processes, a prerequisite is that the physical nature of the H₂O-molecule system is understood. There are many studies that have been published on the system H₂O and the behavior of the H₂O molecule in various chemical and physical environments

(see Ball 1999 or Franks 2000 for an introduction, and Eisenberg and Kauzmann 1969 and Jeffrey 1997 for a more advanced treatment). One of the most important physical aspects that needs to be understood is thermodynamic behavior. In terms of earth science related questions, it is necessary to investigate further how the H₂O molecule interacts with a variety of geomaterials.

Certain minerals offer the possibility for one to study the nature of the H₂O molecule at a relatively simple yet fundamental level, and also to look at how it interacts with crystalline phases as manifested, for example, through its thermodynamic behavior. One such mineral is cordierite. Cordierite of ideal formula, $(\text{Mg,Fe})_2\text{Al}_4\text{Si}_5\text{O}_{18} \cdot x(\text{H}_2\text{O})$, where $x = 0$ to 1, can adsorb

* E-mail: chg@min.uni-kiel.de

or exchange with the environment H₂O molecules into micro-cavities without changing appreciably its structural framework (i.e., there is very little or no change in volume as a function of the H₂O content—Armbruster and Bloss 1982; Boberski and Schreyer 1990; Geiger and Voigtländer 2000; Rahmoun 2005). This behavior is quite unusual and seldom observed in the mineral kingdom. The H₂O molecules occupy small cavities, roughly 6 Å in diameter, occurring along infinite channel ways running parallel to the crystallographic *c* axis (Cohen et al. 1977; Armbruster 1986). The cavities are located between structural rings forming “bottlenecks,” roughly 3 Å in diameter, consisting of six corner-sharing [(Si,Al)O₄]-tetrahedra that build the aluminosilicate framework.

The vibrational behavior of occluded H₂O molecules in cordierite, and the nature of local interactions between them and the aluminosilicate framework, have been studied using polarized single-crystal and powder IR absorption and Raman spectroscopy (Goldman et al. 1977; Kolesov and Geiger 2000b; Geiger and Kolesov 2002; Geiger and Grams 2003), NMR spectroscopy (Tsang and Ghose 1972; Carson et al. 1982), and inelastic neutron scattering (Winkler and Hennion 1994), and, in addition, by ab-initio calculations (Winkler et al. 1994a). These studies have shown that the H₂O molecules have only weak interactions with the framework. It has been concluded that the behavior of the H₂O molecule approaches that of the “free” state such as found in H₂O vapor. It is also dynamically disordered on the picosecond time scale (Winkler et al. 1994b). Thus, cordierite, and isostructural beryl as well (Kolesov and Geiger 2000a), represent a class of microporous hydrous silicates different from the well-known and intensely studied zeolites. The latter are characterized by having H₂O molecules that show measurable hydrogen bonding with their crystal frameworks and/or with each other and also with extra framework cations (Kvick 1986; Kolesov and Geiger 2002, 2006).

Atomistic or molecular-scale behavior determines, of course, the macroscopic thermodynamic properties of cordierite and its *P-T* stability. The only direct calorimetric measurements on synthetic hydrous Mg-cordierite are those of Carey (1993) and Carey and Navrotsky (1992). The former study investigated the heat capacity of various hydrated states of cordierite above 295 K and the latter the enthalpy of dehydration behavior. In addition, Carey (1995) undertook one of the more recent investigations on the thermodynamic mixing behavior of H₂O in cordierite. This problem is important for petrology and geochemistry and, in fact, many studies have tried to determine the thermodynamic properties of hydrous cordierite using primarily phase-equilibrium data (e.g., Strens 1974; Helgeson et al. 1978; Kurepin 1980; Newton and Wood 1979; Martignole and Sisi 1981; Battacharya and Sen 1985; McPhail et al. 1990; Skippen and Gunter 1996; Harley and Carrington 2001). The partial molar quantities of H₂O for different thermodynamic functions were calculated and the physical nature of the H₂O molecule analyzed. There are significant differences in the various calculated thermodynamic functions, such as the entropy, between the different studies. Moreover, from these works it has been proposed that the behavior of the H₂O molecule in cordierite is similar to that in liquid H₂O (Carey 1995) or to that in the zeolites (Newton 1972; Newton and Wood 1979) or is ice-like (Mukhopadhyay and Holdaway 1994), all of which

are in contrast to interpretations based on spectroscopy.

However, there is still a lack of experimental data that prohibits truly quantitative thermodynamic-model formulations and an understanding of the physical nature of the H₂O molecule. In this regard, very importantly, the low-temperature *C_p* behavior of hydrous Mg-cordierite is not known. This information is mandatory if one is to understand the thermodynamic behavior of cordierite and also the nature of the weak interactions between the guest H₂O molecules and the host aluminosilicate framework. Because these interactions are so weak, they will be largely reflected in the nature of the *C_p* behavior at very low temperatures, well below room temperature. Moreover, to obtain the standard third-law entropy of hydrous cordierite,

$$S_o = \int_0^{298.15} \frac{C_p}{T} dT \quad (1)$$

low-temperature heat capacities need to be determined.

We have, therefore, measured, for the first time, *C_p* of a well-characterized synthetic hydrous Mg-cordierite from 6 to 300 K using precise adiabatic calorimetry. This approach allows a more rigorous analysis of the nature and the thermodynamic properties of the H₂O molecule in cordierite, in particular, and in several of micro/nanoporous zeolites as well. Here, the role of hydrogen bonding (e.g., Jeffrey 1997) is important and it receives critical attention.

SYNTHESIS AND SAMPLE CHARACTERIZATION

Approximately 8 g of hydrous cordierite were synthesized using hydrothermal methods. To do this, about 1 g of anhydrous cordierite (for a description of its synthesis and characterization, see Paukov et al. 2006) was placed in a gold capsule of 5 mm diameter and about 3.5 cm length together with about 50 μL of doubly distilled H₂O. The capsules were crimped and welded shut on both sides and then weighed before and after the synthesis experiment to check for water loss and capsule tightness. The experimental synthesis conditions were 4 kbar and 600 °C for 24 hours, and they were carried out in standard cold-seal-type high-pressure vessels. Upon opening most of the capsules, we observed the presence of water. These observations ensured that water-saturated conditions were present during the hydration experiments. Only those syntheses with water present were used in the *C_p* measurements.

One synthesis product was examined by X-ray diffraction (XRD) to check for phase purity and to determine its unit-cell parameters. The synthetic product was white in color and very fine-grained. XRD results showed that only cordierite reflections were present (Fig. 1). A Rietveld refinement was undertaken (see Rahmoun 2005) and the determined unit-cell parameters and the distortion index are very similar [*a* = 17.060(2) Å, *b* = 9.721(1) Å, and *c* = 9.338(1) Å with *V* = 1548.7(3) Å³ and Δ = 0.25] to those of the anhydrous cordierite that was used as a starting material (see Paukov et al. 2006). More information on the synthesis method and characterization can be found in Rahmoun (2005).

To characterize the Class/Type of H₂O present and to determine the H₂O content of the synthetic cordierites quantitatively IR spectroscopy and thermal gravimetric measurements were carried out. An FTIR spectrum (Fig. 2) shows the presence of two H₂O-stretching bands at 3689 (ν₃) and 3595 (ν₁) cm⁻¹, which means that the microcavity H₂O was incorporated as the Class I-Type I variety (Kolesov and Geiger 2000b; see also slightly corrected version in Geiger and Kolesov 2002). IR measurements also showed the presence of very small amounts of molecular H₂O not present in the channel cavities, as evidenced by a broad weak band located around 3400 cm⁻¹. However, it is difficult to determine whether this band reflects H₂O in fluid inclusions in cordierite, H₂O in the KBr, or H₂O occurring on the surfaces of the fine cordierite particles. The IR results were used to calculate the H₂O contents using an unpublished absorption coefficient (Rahmoun 2005) and they show that each lot of synthetic cordierite contained 2.0 ± 0.1 wt% H₂O. In addition to the IR measurements, the H₂O content was determined by three separate thermogravimetric measurements using identical lots of cordierite weighing 180 mg. Two measurements were made using a TG-209 Netzsch thermobalance. Here, the samples were heated to 900 °C with a heating rate of 15 °C/min holding

the sample in a gold crucible in an argon atmosphere. In the third measurement, the mass loss after calcination was determined after heating the sample at 1000 °C for 15 min in a muffle furnace. The H₂O content, as averaged over the three measurements of mass loss, was determined to be $1.95 \pm 0.02\%$. This value is in excellent agreement with the content determined via the IR spectrum. This corresponds to 0.645 ± 0.006 molecules of H₂O per mole of Mg-cordierite. For the first calculations of C_p in our work, the formula for our hydrous cordierite was taken as $\text{Mg}_{1.97}\text{Al}_{3.94}\text{Si}_{5.06}\text{O}_{18} \cdot 0.645 \text{H}_2\text{O}$. Following the C_p measurements and an analysis of the data, the H₂O content was modified (see below). The composition of the cordierite proper, without H₂O, was taken to be the same as that of anhydrous cordierite studied earlier (Paukov et al. 2006).

Heat-capacity measurements and results

The heat-capacity measurements for hydrous Mg-cordierite were made using a vacuum adiabatic calorimeter in 151 experiments at various temperatures between 6 and 299 K. We used the same procedure and the same calorimeter ampoule in which the heat capacity of anhydrous Mg-cordierite was measured (Paukov et al. 2006). The total mass of the hydrous cordierite sample was 6.6422 g. The molar mass was taken as 595.910 g.

The experimental results are presented in Figure 3. For comparison, the $C_p(T)$

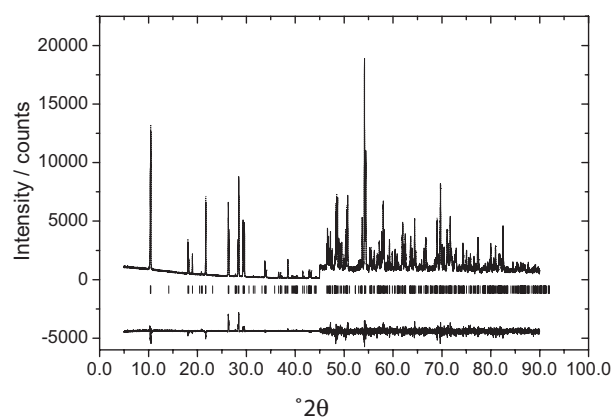


FIGURE 1. Powder X-ray diffraction pattern of synthetic hydrous Mg-cordierite from 5 to 95 °2θ. Note the expanded abscissa for the high-angle data. Only peaks that can be assigned to cordierite are observed. A description of the Rietveld refinement procedure can be found in Rahmoun (2005).

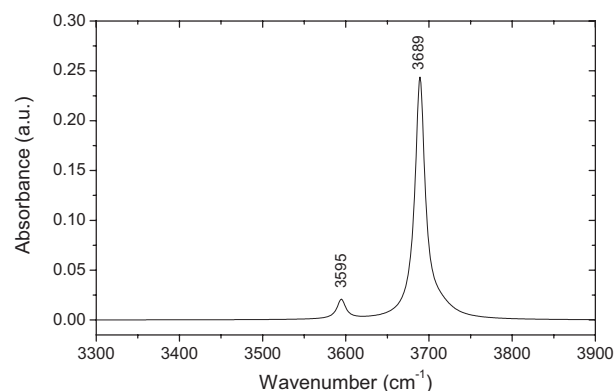


FIGURE 2. Powder IR spectrum of synthetic hydrous Mg-cordierite from 3300 to 3900 cm^{-1} . About 1 mg of cordierite was included in 100 mg of KBr for the measurements. Two internal H₂O stretching bands can be observed at 3689 (ν_3) and 3595 (ν_1) cm^{-1} . Both can be assigned to Class I-Type I H₂O (Kolesov and Geiger 2000b; see also Geiger and Kolesov 2002). A more detailed description of the IR methodology can be found in Rahmoun (2005).

behavior for anhydrous Mg-cordierite (Paukov et al. 2006) is also shown. In the $C_p(T)$ data of hydrous Mg-cordierite, two small anomalies near 273 and 239 K are observed. Using a conventional pulse-heating technique for the heat-capacity determinations, experimental data were collected over 1 to 10 K temperature intervals. Each datum thereby corresponds to a C_p value averaged over the temperature-heating interval. In the case where a heat capacity anomaly is present, more careful investigation is often required. Thus, we used a continuous-heating technique, whereby the calorimeter is heated continuously with a slow heating rate under adiabatic conditions. A computer program records the temperature and the power supplied to the calorimeter at small time intervals and calculates the experimental C_p . Here, the temperature intervals between the experimental data obtained at slow scanning rate are small and the C_p values are, therefore, close to the true value, i.e., $C_p = dH/dT$. This experimental technique was described by Westrum et al. (1968), and later it was essentially developed and employed by Bessergenev et al. (1989, 1992). Using this scanning technique, the temperature maximum of the larger anomaly was determined to be at 272.98 ± 0.03 K (Fig. 4). This anomaly, we think, is related to the melting of ice that occurs in tiny fluid inclusions in the cordierite sample that were formed during hydrothermal synthesis of hydrous cordierite.

In addition to this larger C_p anomaly, a second anomaly is observed at about 239 K. This anomaly was only observable if the calorimeter was first cooled down to temperatures much lower than 239 K followed by heating to this temperature. The anomaly was not observed when approaching this temperature region from higher temperatures. Thus, this C_p -feature appears to mark a first-order-like phase transition having considerable hysteresis. It could possibly be caused by the “melting/freezing” of adsorbed surface H₂O. Clearly, the “melting” point of such H₂O could be 30–40 K lower than that of “normal H₂O.” This anomaly was also studied in detail using the continuous heating technique. The temperature maximum thereby determined was 239.43 ± 0.13 K with a maximal C_p value of 424.9 J/(K·mol).

To determine the heat capacity associated solely with the H₂O molecules in hydrous Mg-cordierite, the difference between the experimental C_p values of hydrous Mg-cordierite and the smoothed C_p values of anhydrous Mg-cordierite must be calculated. When this is done, the small anomalies at about 273 and 239 K become more pronounced (Fig. 5, in this figure, only data obtained by the pulse-heating technique are presented). Because we think that the two small C_p anomalies are not related to H₂O molecules located in the channel cavities of cordierite, it is necessary to correct the heat-capacity data for the effect of this nonchannel H₂O. There are no thermodynamic data for dispersed-surface H₂O, and we assume that its enthalpy of melting is similar to that for “normal H₂O,” that is, $\Delta H = 6010$ J/mol (Glushko et al. 1978). Thus, we attribute the “anomalous part” of the enthalpy occurring between 220 to 280 K to the enthalpy of melting, $\Delta_m H$, of the nonchannel H₂O. In Figure 5, this corresponds to the area between the experimental C_p data in the temperature region 220 to 280 K and the interpolated “regular” C_p curve given by the open circles. The “regular curve” was calculated using the polynomial $C_p(T) = a + bT + cT^2$ (open circles in Fig. 5). $\Delta_m H$ was calculated per mole of total H₂O. Dividing $\Delta_m H$ by the enthalpy of the melting of ice (i.e., 6010 J/mol), we calculated the mole fraction of nonchannel H₂O in our cordierite sample to be 0.03 per mole of H₂O. Because one mole of our Mg-cordierite contains a total of 0.645 H₂O, the actual mole fraction of nonchannel H₂O will be 0.02 per mole of hydrous cordierite. Thus, a correction using 0.02 mol of nonchannel H₂O, corresponding to the heat capacity of normal water (ice), was made using data from Glushko et al. (1978). We note that the correction does not exceed 0.5% for the C_p of hydrous Mg-cordierite over the entire temperature interval studied.

Next, to obtain the heat capacity values for just the molecular H₂O in hydrous Mg-cordierite, the C_p data for anhydrous Mg-cordierite (Paukov et al. 2006) were subtracted from the corrected data for hydrous Mg-cordierite. When the correction for nonchannel H₂O is made, the resulting heat-capacity curve should be smooth, showing no anomalies. Therefore, at temperatures between 220 and 280 K, the heat-capacity values for molecular H₂O were taken from the “regular curve” (shown by open circles in Fig. 5). Similarly, the corrected heat-capacity values for hydrous Mg-cordierite between 220 and 280 K were obtained by calculating the regular $C_p(T)$ curve for hydrous Mg-cordierite after making the correction. It should be noted here that the term “heat capacity” for molecular H₂O is not strictly correct. It means only that part of the heat capacity of hydrous Mg-cordierite that is associated with H₂O molecules, and it is equal to the difference between the heat capacities of hydrous and anhydrous Mg-cordierite, calculated for 1 mol of H₂O.

The heat-capacity data for hydrous Mg-cordierite, corrected for the non-structural H₂O, are given in Table 1. The data correspond to the formula $\text{Mg}_{1.97}\text{Al}_{3.94}\text{Si}_{5.06}\text{O}_{18} \cdot 0.625 \text{H}_2\text{O}$, because a part of the H₂O in hydrous Mg-cordierite is not structural water. The smoothed values of the heat capacity and other thermodynamic functions are listed in Table 2. The smoothed heat capacity values

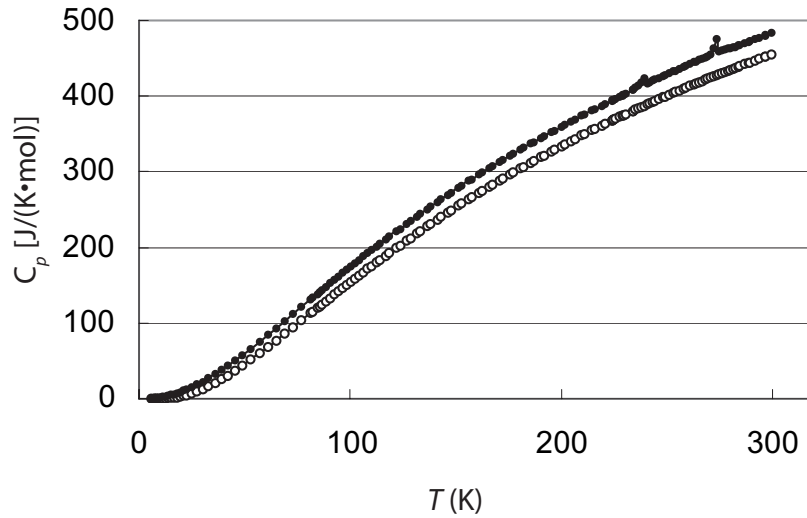


FIGURE 3. Heat capacity of anhydrous (open circles) and hydrous (filled circles) Mg-cordierite.

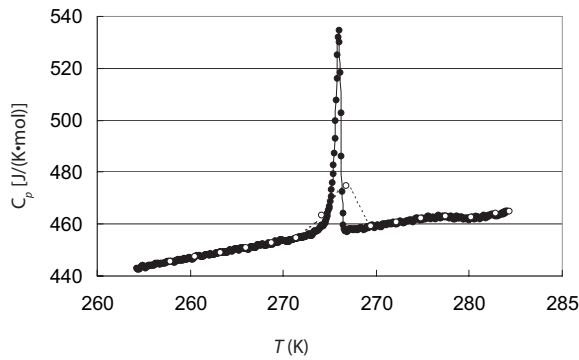


FIGURE 4. Heat capacity of hydrous Mg-cordierite in the temperature vicinity around 273 K; pulse heating (open circles) and continuous heating (filled circles) measurements.

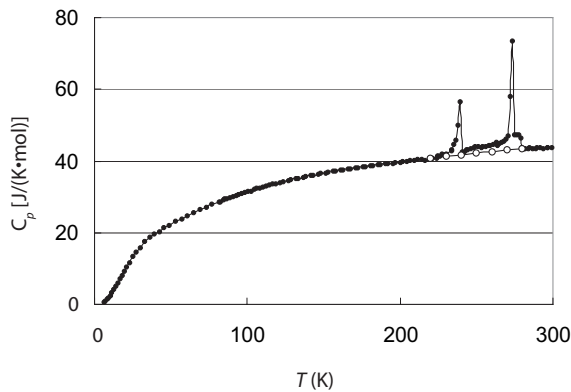


FIGURE 5. Difference between heat capacities of hydrous and anhydrous Mg-cordierite relative to 1 mol of H₂O. Filled circles = experimental data on the heat capacity of total H₂O in the sample; open circles = the regular curve, which corresponds to the C_p of H₂O between 220 and 280 K if there are no anomalies.

for molecular H₂O in hydrous Mg-cordierite are presented in Table 3. With regard to the precision of our thermodynamic data, it should be noted that the observed C_p anomalies relate to very small amounts of water—only about 3% of the total amount of the H₂O molecules in the channels. Their contribution to the other thermodynamic properties of hydrous Mg-cordierite is negligible. For example, their enthalpy contribution to the total of the enthalpy of hydrous Mg-cordierite at 298.15 K is less than 0.2% and only about 2% for the enthalpy of the H₂O molecules at the same temperature. We estimate the precision of our heat-capacity data for molecular H₂O in hydrous Mg-cordierite to be between 3 and 5%, after taking into account scatter in the experimental data for both anhydrous and hydrous Mg-cordierites, the uncertainties in our correction, and the uncertainty connected with calculating the “regular” C_p curves.

Our low-temperature C_p results can be compared with those of Carey (1993), which were obtained by DSC methods on several hydrous Mg-cordierites having different H₂O contents at temperatures above 295 K. To do this, the data of Carey (1993) were interpolated to obtain C_p values corresponding to the H₂O content in our sample. The results of the calculation show that agreement between both sets of calorimetric measurements is very good; the difference is less than 0.3% (Fig. 6).

TABLE 1. Experimental heat capacities of hydrous Mg-cordierite of composition Mg_{1.97}Al_{3.94}Si_{5.06}O₁₈·0.625H₂O corrected for non-structural H₂O

T (K)	C _{p,m} (T) [J/(K·mol)]	T (K)	C _{p,m} (T) [J/(K·mol)]	T (K)	C _{p,m} (T) [J/(K·mol)]
6.12	0.4692	94.40	161.02	182.12	330.92
7.13	0.6971	96.42	165.62	185.35	336.06
8.23	1.0471	98.32	169.90	186.95	338.65
9.26	1.4376	100.36	174.47	190.19	343.71
10.34	1.9249	102.28	178.68	191.77	346.20
11.41	2.4739	104.36	183.27	195.04	351.11
12.66	3.2438	106.24	187.49	196.60	353.60
13.92	4.0733	108.34	192.00	199.89	358.42
15.19	4.9438	110.20	195.93	201.44	360.83
16.45	5.9215	112.33	200.57	204.75	365.77
17.90	7.1686	114.16	204.45	206.27	368.12
19.49	8.6651	116.77	209.95	209.60	372.93
21.09	10.331	118.64	213.88	211.11	375.08
22.72	12.191	121.72	220.30	214.47	379.82
24.90	14.927	123.59	224.20	215.97	381.82
27.54	18.458	126.65	230.37	219.29	386.44
30.13	22.250	128.48	234.05	220.00	387.56
32.98	27.017	131.59	240.29	230.00	401.08
36.07	32.338	133.33	243.73	240.00	414.01
39.15	37.947	136.55	250.01	250.00	426.45
42.24	43.625	138.20	253.17	260.00	438.42
45.31	49.802	141.47	259.45	270.00	449.91
48.89	57.198	143.11	262.64	280.00	460.93
52.99	66.021	146.42	268.87	280.06	461.07
57.03	74.858	147.98	271.77	281.39	462.30
61.02	83.910	151.39	278.06	282.13	463.20
65.00	93.101	152.88	280.79	283.63	464.76
68.97	102.36	156.30	287.05	284.52	465.86
72.97	111.63	157.77	289.66	286.92	468.20
76.97	120.86	161.19	295.75	288.50	469.86
81.39	131.10	162.63	298.25	289.41	470.97
82.45	133.51	166.06	304.15	291.75	473.33
84.43	138.10	167.55	306.72	293.55	475.04
85.38	140.43	170.86	312.34	296.47	478.19
86.46	142.88	172.40	314.91	296.62	478.42
88.44	147.37	175.65	320.37	299.39	481.28
90.47	151.99	177.23	322.95		
92.47	156.59	180.50	328.29		

TABLE 2. Thermodynamic properties of hydrous Mg-cordierite of composition $\text{Mg}_{1.97}\text{Al}_{3.94}\text{Si}_{5.06}\text{O}_{18}\cdot 0.625\text{H}_2\text{O}$

T (K)	$C_p^{\circ}(T)$ [J/(K·mol)]	$S_m^{\circ}(T) - S_m^{\circ}(0)$ [J/(K·mol)]	$H_m^{\circ}(T) - H_m^{\circ}(0)$ (J/mol)	$\Phi_m^{\circ}(T)$ [J/(K·mol)]
6	0.4387	0.1496	0.6717	0.0376
10	1.771	0.6418	4.749	0.1669
15	4.802	1.886	20.60	0.5127
20	9.210	3.838	55.05	1.085
25	15.03	6.492	115.1	1.890
30	22.14	9.842	207.5	2.926
35	30.34	13.86	338.2	4.193
40	39.39	18.49	512.2	5.685
45	49.16	23.69	733.3	7.391
50	59.54	29.40	1005	9.303
60	81.61	42.18	1709	13.69
70	104.7	56.49	2640	18.77
80	127.9	71.98	3803	24.44
90	151.0	88.38	5198	30.63
100	173.6	105.5	6821	37.25
120	216.7	141.0	10730	51.56
140	256.7	177.4	15470	66.93
160	293.6	214.2	20980	83.04
180	327.5	250.7	27190	99.64
200	358.7	286.9	34060	116.6
220	387.7	322.4	41530	133.7
240	414.1	357.3	49550	150.9
260	438.4	391.4	58080	168.1
280	460.9	424.7	67070	185.2
298.15	480.0 ± 1.9	454.3 ± 1.8	75610 ± 300	200.7 ± 0.8
299.39	481.3	456.3	76210	201.7

Note: $\Phi_m^{\circ}(T) = S_m^{\circ}(T) - S_m^{\circ}(0) - [H_m^{\circ}(T) - H_m^{\circ}(0)]/T$.

TABLE 3. Heat capacity of molecular H_2O in hydrous Mg-cordierite of composition $\text{Mg}_{1.97}\text{Al}_{3.94}\text{Si}_{5.06}\text{O}_{18}\cdot 0.625\text{H}_2\text{O}$

T (K)	$\Delta C_m(T)$ [J/(K·mol)]
6.12	0.649
10	2.36
15	5.99
20	9.93
25	13.5
30	16.3
35	18.6
40	20.3
45	21.7
50	22.9
60	25.0
70	27.0
80	28.7
90	30.3
100	31.7
120	34.2
140	36.0
160	37.6
180	38.7
200	39.7
220	40.5
240	41.1
260	41.6
280	42.0
298.15	42.2 ± 2.1
299.39	42.3

Note: It is given by $\Delta C_m(T) = [C_p^{\circ}(T)$ (hydrous cordierite) - $C_p^{\circ}(T)$ (anhydrous cordierite)]/0.625.

DISCUSSION

The vibrational behavior of the H_2O molecule and calculations on the heat capacity of H_2O in Mg-cordierite at $T < 300$ K

The vibrational properties of the H_2O molecule in cordierite have received considerable attention in the literature, but nevertheless there appears to be uncertainty and a lack of understanding surrounding its behavior. In principle, an H_2O

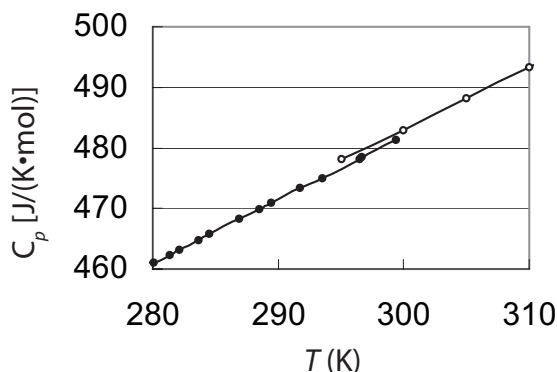
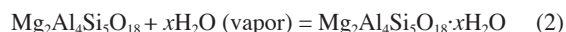


FIGURE 6. Adiabatic calorimetric data for the heat capacity of hydrous Mg-cordierite compared with the DSC measurements of Carey (1993) made at higher temperature: filled circles = this study, open circles = data of Carey (1993).

molecule should have nine vibrational modes that include three internal vibrations at high energies, and three external translations, and three external rotations (or librations) that occur at lower energies (Eisenberg and Kauzmann 1969). The various mode energies change depending on the environment in which the H_2O is located, and Eisenberg and Kauzmann (1969) discuss them for solid, liquid, and gaseous H_2O states. In his analysis of some of the first spectra recorded on hydrous beryl and cordierite, Strens (1974) concluded that only one rotational (i.e., librational) H_2O mode is active and that the three translational modes are quenched. He made a “first-order calculation” for the entropy of reaction:



With $x = 1$, a value of 25 J/(mol·K) at 298 K and 1 bar was obtained by Strens. Using the data from the present study and from Paukov et al. (2006), and S_0 (298.15 K) for H_2O vapor from Robie and Hemingway (1995), we calculated a value of -108.3 J/(mol·K). Carey (1995) obtained a value of -108.2 ± 3.2 J/(mol·K) using published phase-equilibrium data on the hydration states of Mg-cordierite at different P and T . The agreement between independent and different experimental methods (i.e., calorimetry and phase-equilibrium study) is excellent. Subsequent to the work of Strens, spectroscopic measurements have shown that several of the external H_2O modes of hydrous Mg-cordierite can be observed (Winkler and Hennion 1994; and for the case of beryl see Kolesov and Geiger 2000a).

Carey (1993) presented, following upon the work of Barrer (1978), a “statistical-mechanical” model to interpret the C_p behavior of H_2O in Mg-cordierite at $T > 300$ K. The nature of his arguments regarding the vibrational behavior are not completely clear to us, but it is reasoned that four external modes of the H_2O molecule are present and that two others have been lost and taken up by low-frequency vibrational modes associated with the crystal lattice. The model predicts that the heat capacity for $\text{Mg}_2\text{Al}_4\text{Si}_5\text{O}_{18} \cdot \text{H}_2\text{O}$ at $T > 300$ K can be described approximately by the value of the gas constant $R = 8.314$ J/(mol·K). We argue here that there is no reason to assume, a priori, that external H_2O

modes are “quenched” or “lost” or taken up by lattice vibrational modes (of course, there may be some degree of coupling between H₂O molecular modes and lattice modes, but based on the various published spectra, they must be weak). Thus, we present a new and further analysis of the vibrational and heat-capacity behavior of the H₂O molecule in hydrous Mg-cordierite.

Low-temperature heat-capacity behavior is strongly a function of the phonon density of states in the low-energy region, and here the external modes of the H₂O in the channel cavities must be carefully considered. The question arises if it is possible to model the experimental calorimetric data by undertaking calculations to understand better the physical nature of the H₂O molecule in hydrous Mg-cordierite. First, the low-energy vibrational and dynamic behavior of H₂O molecules in cordierite was investigated by using inelastic neutron (Winkler and Hennion 1994) and quasi-elastic neutron scattering (Winkler et al. 1994b). In the first work, they assigned two bands at 6 and 10 meV in their spectra to translational motions of the H₂O molecule and a broad band at 27 meV to a librational motion. Because the H₂O molecule-framework interaction is so weak (Langer and Schreyer 1976; Winkler et al. 1994a; Kolesov and Geiger 2000b), one can, as a first-order approximation, consider these external vibrational modes of H₂O as independent oscillators, and one can calculate model heat capacities under different mode assumptions using the Einstein function. Figure 7 shows the results of this exercise. The curve marked by the filled triangles corresponds to a calculation based on just two translational modes with energies of 6 and 10 meV and one librational mode at 27 meV, as observed in the spectra (their Einstein temperatures, Θ_E , are 70, 116, and 313 K, respectively). Clearly, such a model does not reproduce the experimental C_p data; thus we made further calculations. Winkler and Hennion (1994) suggested that the slightly broadened peak related to an H₂O translation at 10 meV could actually consist of two closely spaced vibrational modes. Further calculations including two translation modes at 116 K, plus the ones at 70 and 313 K (i.e., a total of four modes), showed that heat capacity values increase between 100 and 300

K (results not shown in Fig. 7). However, including this third translational mode at 116 K does not contribute greatly to C_p at lower temperatures and, thus, agreement between calculation and experiment is still poor.

To obtain better agreement between experimental and model heat capacity values at $T < 30$ K, it is necessary to have a translational mode with a corresponding Θ_E value considerably lower than the lowest energy mode observed in the inelastic neutron-scattering experiments. Reasonable agreement between experimental and model heat capacity values at $T < 30$ K can be obtained when a hypothetical external H₂O translational mode, corresponding to a value of $\Theta_E = 45$ K, is incorporated into the calculations. The value of $\Theta_E = 45$ K could possibly correspond to the small peak at 48 K (1 THz) observed by Winkler and Hennion (1994) in their measurements, but they attributed it to contamination. [Here, it should be stated that if one accepts the occurrence of a third translational mode with a value corresponding to $\Theta_E = 45$ K, the presence of two closely spaced modes at 116 K (10 meV) is not possible, because the H₂O molecule should have only three translations. Furthermore, based on simple crystal-chemical considerations, we consider it unlikely that two translational modes, so closely spaced in energy, are present in the vibrational spectrum because the two longest dimensions in the channel cavities are different along a and b —about 6.0 and 5.4, respectively. Accordingly, H₂O translational modes, in which the H₂O molecule vibrates against the cavity walls, should be somewhat dissimilar in energy.] The calculated curve obtained using three translational modes at 45, 70, and 116 K and one librational mode at 313 K is marked by plus signs (+) in Figure 7. This calculated curve agrees well with experimental data at low temperatures, but is too low at 100 to 300 K.

This result is understandable, because the H₂O molecule should have three librational modes, but we used only one (i.e., 313 K) in our model calculations. Thus, we made yet another calculation using a second librational mode. Winkler and Hennion (1994) noted the presence of weak features in their spectra located between 15–25 meV, which may be related to a second librational mode. The weak feature in their spectrum near 22 meV corresponds to $\Theta_E = 255$ K. Repeating the calculation using three translational modes (45, 70, and 116 K), and also with two librational modes (255 and 313 K), improves the agreement with experimental data greatly (Fig. 7, curve marked by open circles). We conclude that the question of the presence of a third librational H₂O mode, as well as the presence of a low energy translation, requires further spectroscopic study.

Analysis of the thermodynamic properties of hydrous Mg-cordierite

There have been several studies directed toward obtaining thermodynamic data for hydrous Mg-cordierite (e.g., Kurepin 1980; Helgeson et al. 1978; Newton and Wood 1979; Martignole and Sisi 1981; Battacharya and Sen 1985; McPhail et al. 1990; Skippen and Gunter 1996; Harley and Carrington 2001). The different functions (G , H , S , and V) that have been obtained are largely based on phase-equilibrium data and model calculations. There is a significant discrepancy among the various values from the different investigations (Table 4). This has given rise to, for example, conflicting thermodynamic descriptions for the

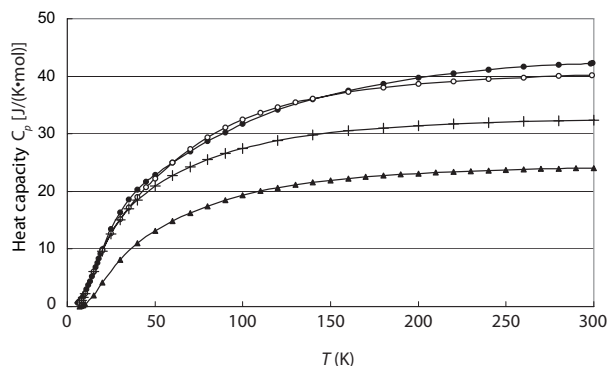


FIGURE 7. Various model heat capacities for molecular H₂O in cordierite calculated using the Einstein function: filled circles = experimental data, and filled triangles = model heat capacities calculated using the three modes observed in inelastic neutron-scattering spectra at 70, 116, and 313 K (Winkler and Hennion 1994). Model heat capacities calculated using four (plus signs) (45, 70, 116, and 313 K) and five (open circles) external H₂O modes (45, 70, 116, 255, and 313 K), respectively.

thermodynamic hydration state as a function of P and T (i.e., phase diagram). The calorimetric and XRD results of this study should help clear up some of the confusion and uncertainty and provide for more rigorous thermodynamic calculations.

First, the XRD data obtained from this study and that of Paukov et al. (2006), which used an anhydrous cordierite sample that was hydrated for this study, show that there is very little to no volume change in Mg-cordierite with the incorporation of H_2O at 1 atm. The volume of anhydrous and hydrous cordierite do not show experimentally significant differences in their molar volumes, as also indicated from data published in other studies (Armbruster and Bloss 1982; Geiger and Voigtländer 2000). We conclude that the partial molar volume of H_2O in cordierite is zero at 1 atm. Bhattacharya and Sen (1985) and McPhail et al. (1990) concluded from phase-equilibrium data obtained at different pressures that it is nonzero.

Second, our data permit a determination of the partial molar entropy of H_2O in Mg-cordierite and/or the entropy of reaction 2. Using the data in Table 3 and assuming that there is ideal mixing of H_2O in Mg-cordierite, we calculated a partial molar entropy for one mole of H_2O in Mg cordierite at 298.15 K and 1 bar as 80.5 J/(mol·K). This value is in excellent agreement with that calculated by Carey (1995) from phase-equilibrium data.

Some thoughts on the heat-capacity behavior of H_2O in cordierite, selected zeolites, and the system H_2O : Microscopic-macroscopic relationships

The structures and vibrational energies of gaseous, liquid, and solid-state H_2O systems are discussed in Eisenberg and Kauzmann (1969). An important physical difference between liquid and solid H_2O , and gaseous H_2O (steam), is the presence of hydrogen bonding in the first two phases. Indeed, hydrogen bonding plays a central role in determining the physical and chemical properties of the H_2O system (Eisenberg and Kauzmann 1969; Jeffrey 1997; Ball 1999; Franks 2000). For this reason, it must be given careful consideration in hydrous, H_2O -bearing minerals.

In Figure 8, the heat-capacity behavior for H_2O in cordierite is compared with that for H_2O in the zeolites analcime, $NaAlSi_3O_6 \cdot H_2O$ (Johnson et al. 1982), mordenite, $(Ca, Na_2, K_2) Al_2Si_{10}O_{24} \cdot 7H_2O$ (Johnson et al. 1992), and parnatrolite,

$Na_2Al_2Si_3O_{10} \cdot 3H_2O$ (Paukov et al. 2002) at $T < 300$ K. It is evident that the heat-capacity behavior for the H_2O molecule in Mg-cordierite differs fundamentally from its behavior in the other micro/nanoporous phases. We interpret the macroscopic thermodynamic data in terms of the local vibrational and energetic behavior of the H_2O molecule in these phases as follows: The H_2O molecule in synthetic Mg-cordierite is “quasi-free” in terms of its vibrational properties and it has weak interactions with the aluminosilicate framework (Langer and Schreyer 1976; Winkler et al. 1994a, 1994b; Kolesov and Geiger 2000b; Geiger and Kolesov 2002; Geiger and Grams 2003—cf. Stout 1975; Carey and Navrotsky 1992; Carey 1995). This behavior is clearly reflected on a local scale, for example, in the IR or Raman spectra by the wavenumber and form of the internal H_2O stretching bands (e.g., Fig. 2). That is, these bands are relatively narrow compared with those in liquid H_2O and ice (Eisenberg and Kauzmann 1969), for example. More importantly, they occur at higher wavenumbers than the stretching modes in these two phases and also compared to the internal H_2O stretching modes observed in the spectra of zeolites (Kolesov and Geiger 2002, 2006). Furthermore, the H_2O molecule in cordierite is dynamically disordered (Aines and Rossman 1984; Kolesov and Geiger 2000b), even down to 3 K, at the pico-second time scale as shown by quasi-elastic, neutron-scattering measurements (Winkler et al. 1994b). Of course, the heat-capacity behavior of the H_2O molecules at low temperatures (i.e., $T < 100$ K) demonstrates that they are not completely free and a strict comparison to their behavior in an ideal gas is not valid. Some interactions of H_2O molecules with the cordierite framework are present, but they

TABLE 4. Partial molar volume, V_i , and partial molar entropy, S_i , of H_2O in hydrous Mg-cordierite at 1 bar and 298 K from various studies

Study	V_i (cc/mol)	S_i [J/(mol·K)]
This study	0.0	80.5
Kurepin (1980)	—	≈ 120
Helgeson et al. (1978)	8.00	56.40
Geiger and Voigtländer (2000)	0	—
Harley and Carrington (2001)	0	97.69
Carey (1995)	0	80.6
Newton and Wood (1979)	—	69.8
McPhail et al. (1990)*	23.066	156.665

* $Mg_2Al_4Si_2O_{18} \cdot 2H_2O - Mg_2Al_4Si_3O_{18}$.

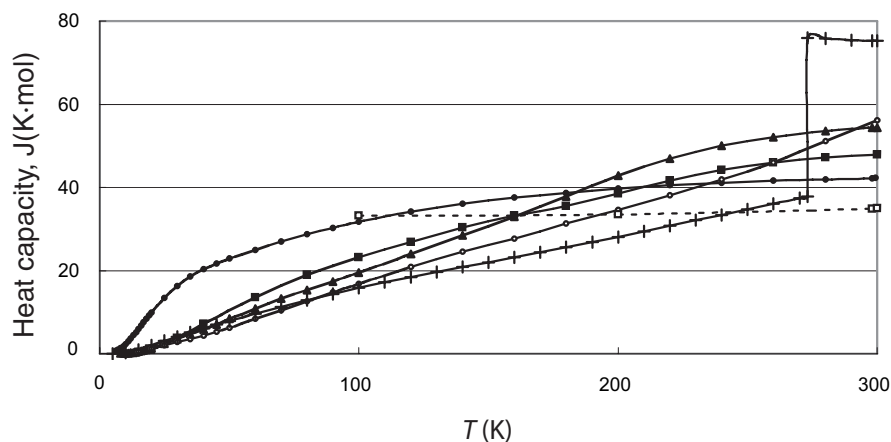


FIGURE 8. Heat capacity of molecular H_2O in various micro/nanoporous hydrous silicates and ice, liquid, and gaseous H_2O : filled circles = cordierite, filled squares = analcime, filled triangles = mordenite, open circles = parnatrolite, plus signs = ice and liquid water, and open squares = gaseous H_2O .

are much weaker than the hydrogen bonding that is present in ice or liquid H₂O and also in zeolites.

The H₂O molecule(s) in zeolites, in contrast to the H₂O in alkali-free cordierite (Geiger and Grams 2003), is/are bonded to an alkali or alkaline-earth cation in the zeolite channels and, in addition, they show measurable hydrogen bonding to their aluminosilicate frameworks and/or to other H₂O molecules. The hydrogen bonding is evidenced in both diffraction experiments (e.g., Kvik 1986) and more clearly and quantitatively in various types of vibrational spectra (e.g., Jobic 1992; Line and Kearley 2000; Winkler and Hennion 1994; Winkler et al. 1994b; Kolesov and Geiger 2002, 2006). The behavior of the H₂O molecule in cordierite, and also beryl (Kolesov and Geiger 2000a), is therefore, in this respect, fundamentally different than that in other micro/nanoporous silicates. The H₂O molecule in cordierite is neither zeolite-like in nature nor is its structural environment like that in liquid H₂O or ice. The energies of the external H₂O modes are also affected (see above). The Raman spectra of beryl show librational modes around 200 cm⁻¹ and a translational mode around 10 cm⁻¹, whereas Kolesov and Geiger (2006) showed that translational H₂O modes for three zeolites lie at higher wavenumbers.

Carey (1993) analyzed the C_p behavior of H₂O in cordierite, beryl, several zeolites, H₂O liquid, and H₂O steam at $T > 300$ K using his empirical statistical-mechanical model (his Fig. 4). We present here a simple first-order reinterpretation of these data (a detailed analysis is well beyond the scope of this work because it will require more spectroscopic and lattice-dynamic study). Because of the nature of Boltzmann statistics and statistical mechanics, at $T > 300$ K the energies of the internal H₂O stretching modes in the various phases will make a greater contribution to C_p , in contrast to the situation discussed above for $T < 300$ K. Thus, we propose that the larger heat capacity for molecular H₂O in zeolites compared to the situation in beryl and cordierite at $T > 300$ K is related to the presence of stronger hydrogen bonding in the zeolites (we recognize that interactions of the H₂O molecules with the extra framework cations in the zeolites will also influence the vibrational and energetic behavior of the H₂O molecules, but they will be neglected in this first-order analysis).

Furthermore, the heat capacity for liquid H₂O is greater than that for H₂O in zeolites because here, once again, hydrogen bonding is stronger. Unlike the behavior of high-energy H₂O stretching modes, which decrease in energy with increasing hydrogen bonding strength, the low-energy translational H₂O modes increase in energy with increasing hydrogen bonding in the case of several micro/nanoporous silicates, as well as in ice and liquid H₂O (Kolesov and Geiger 2006). Thus, H₂O in cordierite has a higher C_p than that of H₂O in zeolites or even ice at $T < 150$ K. Concluding, it is the energies of the internal and external H₂O modes that are measurably affecting the C_p behavior in these phases and they are a function of the hydrogen bonding.

The local-bonding properties between the H₂O molecule and the cordierite framework are reflected further in the nature of the macroscopic volume behavior of cordierite upon dehydration or adsorption of H₂O. Here, it has been shown that very little to no volume change occurs with introduction or removal of the H₂O molecule in the structural cavities (Armbruster and Bloss 1982; Geiger and Voigtländer 2000; Rahmoun 2005). This is not the

case for many zeolites (Bish and Carey 2001).

More low-temperature C_p measurements on other H₂O-bearing micro/nanoporous silicates (hemi-morphite, lawsonite, zeolites), in combination with vibrational spectroscopic measurements, are required before a more fundamental and quantitative physical understanding of the nature of the H₂O molecule in minerals can be reached.

ACKNOWLEDGMENTS

We thank Boris A. Kolesov for discussions and W.A. Drebuschak for the thermogravimetric measurements and helpful advice. J.W. Carey made a careful review of the manuscript that led us to consider further the thermodynamic behavior of hydrous cordierite. This work was supported by the Integration Interdisciplinary Project no. 81 of the Siberian Branch of the Russian Academy of Sciences and a grant, Ge 659/6-2, from the Deutsche Forschungsgemeinschaft.

REFERENCES CITED

- Aines, R.D. and Rossman, G.R. (1984) The high temperature behavior of water and carbon dioxide in cordierite and beryl. *American Mineralogist*, 69, 319–327.
- Armbruster, T. (1986) Role of Na in the structure of low-cordierite: A single-crystal X-ray study. *American Mineralogist*, 71, 746–757.
- Armbruster, T. and Bloss, F.D. (1982) Orientation and effects of channel H₂O and CO₂ in cordierite. *American Mineralogist*, 67, 284–291.
- Ball, P. (1999) *A biography of water: life's matrix*, 417 p. Farrar, Straus, and Giroux, New York.
- Barrer, R.M. (1978) *Zeolites and clay minerals as sorbents and molecular sieves*, 497 p. Academic Press, London.
- Battacharya, A. and Sen, S.K. (1985) Energetics of hydration of cordierite and water barometry in cordierite-granulites. *Contributions to Mineralogy and Petrology*, 89, 370–378.
- Bessergenev, V.G., Kovalevskaya, Yu.A., Paukov, I.E., and Shkredov, Yu.A. (1989) Heat capacity measurements under continuous heating and cooling using vacuum adiabatic calorimetry. *Thermochimica Acta*, 139, 245–256.
- Bessergenev, V.G., Kovalevskaya, Yu.A., Paukov, I.E., Starikov, M.A., Oppermann, H., and Reichelt, W. (1992) Thermodynamic properties of MnMoO₄ and Mn₂Mo₃O₈. *Journal of Chemical Thermodynamics*, 24, 85–98.
- Bish, D.L. and Carey, J.W. (2001) Thermal behavior of natural zeolites. In D.L. Bish and D.W. Ming, Eds., *Natural Zeolites: Occurrence, Properties, Applications*, 45, p. 403–452. Reviews in Mineralogy and Geochemistry, Mineralogical Society of America, Chantilly, Virginia.
- Boberski, C. and Schreyer, W. (1990) Synthesis and water contents of Fe²⁺-bearing cordierites. *European Journal of Mineralogy*, 2, 565–584.
- Carey, J.W. (1993) The heat capacity of hydrous cordierite above 295 K. *Physics and Chemistry of Minerals*, 19, 578–583.
- (1995) A thermodynamic formulation of hydrous cordierite. *Contributions to Mineralogy and Petrology*, 119, 155–165.
- Carey, J.W. and Navrotsky, A. (1992) The molar enthalpy of dehydration of cordierite. *American Mineralogist*, 77, 930–936.
- Carson, D.G., Rossman, G.R., and Vaughan, R.W. (1982) Orientation and motion of water molecules in cordierite: A proton nuclear magnetic resonance study. *Physics and Chemistry of Minerals*, 8, 14–19.
- Cohen, J.P., Ross, F.K., and Gibbs, G.V. (1977) An X-ray and neutron diffraction study of hydrous low cordierite. *American Mineralogist*, 62, 67–78.
- Eisenberg, D. and Kauzmann, W. (1969) *The structure and properties of water*, 296 p. Oxford University Press, U.K.
- Franks, F. (2000) *Water: 2nd Edition—A Matrix of Life*, 225 p. The Royal Society of Chemistry, Cambridge.
- Geiger, C.A. and Grams, M. (2003) Cordierite IV: Structural heterogeneity and energetics of natural Mg-Fe solid solutions. *Contributions to Mineralogy and Petrology*, 145, 752–764.
- Geiger, C.A. and Kolesov, B.A. (2002) Microscopic-macroscopic relationships in silicates: Examples from IR and Raman spectroscopy and heat capacity measurements. In C.-M. Gramaccioli, Ed., *European Notes in Mineralogy—Energy Modelling in Minerals*, 4, p. 347–387. Eötvös University Press, Budapest, Hungary.
- Geiger, C.A. and Voigtländer, H. (2000) Heat capacity measurements on synthetic Mg- and Fe-cordierite. *Contributions to Mineralogy and Petrology*, 138, 46–50.
- Goldman D.S., Rossman, G.R., and Dollase, W.A. (1977) Channel constituents in cordierite. *American Mineralogist*, 62, 1144–1157.
- Glushko, V.P., Gurvich, L.V., Bergman, G.A., Veitz, I.V., Medvedev, V.A., Khachkuruzov, G.A., and Yungman, V.S., Eds. (1978) *Handbook of "Thermodynamic properties of individual substances," 1*, p. 310. Nauka, Moscow (in Russian).
- Harley, S.L. and Carrington, D.P. (2001) The distribution of H₂O between cordierite and granitic melt: H₂O incorporation in cordierite and its application

- to high-grade metamorphism and crustal anatexis. *Journal of Petrology*, 42, 1595–1620.
- Helgeson, H.C., Delany, J.M., Nesbitt, H.W., and Bird, D.K. (1978) Summary and critique of the thermodynamic properties of rock-forming minerals. *American Journal of Science*, 278-A, 1–229.
- Jeffrey, G.A. (1997) *An introduction to hydrogen bonding*, 303 p. Oxford University Press, New York.
- Jobic, H. (1992) Molecular motions in zeolites. *Spectrochimica Acta*, 48A, 293–312.
- Johnson, G.K., Flotow, H.E., O'Hare, P.A.G., and Wise, W.S. (1982) Thermodynamic studies of zeolites: analcime and dehydrated analcime. *American Mineralogist*, 67, 736–748.
- Johnson, G.K., Tasker, I.R., Flotow, H.E., O'Hare, P.A.G., and Wise, W.S. (1992) Thermodynamic studies of mordenite, dehydrated mordenite, and gibbsite. *American Mineralogist*, 77, 85–93.
- Kolesov, B.A. and Geiger, C.A. (2000a) A single-crystal Raman study of the orientation and vibrational states of molecular water in synthetic beryl. *Physics and Chemistry of Minerals*, 27, 557–564.
- — — (2000b) Cordierite II: The role of CO₂ and H₂O. *American Mineralogist*, 85, 1265–1274.
- — — (2002) Raman spectroscopic study of H₂O in bikitaite: "One-dimensional" ice. *American Mineralogist*, 87, 1426–1431.
- — — (2006) Behavior of H₂O molecules in the channels of natrolite and scolecite: A Raman and IR spectroscopic investigation of hydrous microporous silicates. *American Mineralogist*, 91, 1039–1048.
- Kurepin, V.A. (1980) Thermodynamics of hydrous cordierite, and mineral equilibria involving it. *Geochemistry International*, 34–44. Translation from *Geokhimiya* (1979), 1, 49–60.
- Kvick, A. (1986) Hydrogen bonding in zeolites. *Transactions of the American Crystallographic Association, American Crystallographic Association*, 22, 97–105.
- Langer, K. and Schreyer, W. (1976) Apparent effects of molecular water on the lattice geometry of cordierite: a discussion. *American Mineralogist*, 61, 1036–1040.
- Line, C.M.B. and Kearley, G.J. (2000) An inelastic incoherent neutron scattering study of water in small-pored zeolites and other water-bearing minerals. *Journal of Chemical Physics*, 112, 9058–9067.
- Martignole, J. and Sisi, J.-C. (1981) Cordierite-garnet-H₂O equilibrium: A geological thermometer, barometer, and water fugacity indicator. *Contributions to Mineralogy and Petrology*, 77, 38–46.
- McPhail, D.C., Berman, R.G., and Greenwood, H.J. (1990) Experimental and theoretical constraints on aluminum substitution in magnesian chlorite, and a thermodynamic model for H₂O in magnesian cordierite. *Canadian Mineralogist*, 28, 859–874.
- Mukhopadhyay, B. and Holdaway, M.J. (1994) Cordierite-garnet-sillimanite-quartz equilibrium: I. New experimental calibration in the system FeO-Al₂O₃-SiO₂-H₂O and certain *P-T-X*_{H₂O} relations. *Contributions to Mineralogy and Petrology*, 116, 462–472.
- Newton, R.C. (1972) An experimental determination of the high-pressure stability limits of magnesian cordierite under wet and dry conditions. *Journal of Petrology*, 80, 398–402.
- Newton, R.C. and Wood, B.J. (1979) Thermodynamics of water in cordierite and some petrologic consequences of cordierite as a hydrous phase. *Contributions to Mineralogy and Petrology*, 68, 391–405.
- Paukov, I.E., Moroz, N.K., Kovalevskaya, Yu.A., and Belitsky, I.A. (2002) Low-temperature thermodynamic properties of disordered zeolites of the natrolite group. *Physics and Chemistry of Minerals*, 29, 300–306.
- Paukov, I.E., Kovalevskaya, Yu.A., Rahmoun, N.S., and Geiger, C.A. (2006) A low-temperature heat capacity study of synthetic anhydrous Mg-cordierite (Mg₂Al₄Si₄O₁₈). *American Mineralogist*, 91, 35–38.
- Rahmoun, N.-S. (2005) *Volatile in Cordierit: FT-IR-spektroskopische und thermoanalytische Untersuchungen*, 182 p. Ph.D.thesis, Universität Kiel, Germany.
- Robie, R.A. and Hemingway, B.S. (1995) Thermodynamic properties of minerals and related substances at 298.15 K and 1 bar (10⁵ Pascals) pressure and at higher temperatures. *Geological Survey Bulletin*, 2131, 461 p.
- Skippen, G.B. and Gunter, A. E. (1996) The thermodynamic properties of H₂O in magnesium and iron cordierite. *Contributions to Mineralogy and Petrology*, 124, 82–89.
- Stout, J.H. (1975) Apparent effects of molecular water on the lattice geometry of cordierite. *American Mineralogist*, 60, 229–234.
- Strens, R.G.J. (1974) The common chain, ribbon, and ring silicates. In V.C. Farmer, Ed., *The Infrared Spectra of Minerals*, p. 285–330. Bartholomew Press, Dorking, Surrey, U.K.
- Tsang, T. and Ghose, S. (1972) Nuclear magnetic resonance of ¹H and ²⁷Al and the Al-Si order in low cordierite. *Journal of Chemical Physics*, 56, 3329–3332.
- Westrum, E.F., Jr., Furukawa, G.T., and McCullough, G.P. (1968) Adiabatic low-temperature calorimetry. In G.P. McCullough and D.W. Scott, Eds., *Experimental Thermodynamics, Vol. 1, Calorimetry of non-reacting systems*, p. 133–214. Butterworth's and Co., London.
- Winkler, B. and Hennion, B. (1994) Low-temperature dynamics of molecular H₂O in bassanite, gypsum, and cordierite investigated by high resolution incoherent inelastic neutron scattering. *Physics and Chemistry of Minerals*, 21, 539–545.
- Winkler, B., Milman, V., and Payne, M.C. (1994a) Orientation, location, and total energy of hydration of channel H₂O in cordierite investigated by ab-initio total energy calculations. *American Mineralogist*, 79, 200–204.
- Winkler, B., Coddens, G., and Hennion, B. (1994b) Movement of channel H₂O in cordierite observed with quasi-elastic neutron scattering. *American Mineralogist*, 79, 801–808.

MANUSCRIPT RECEIVED MARCH 9, 2006

MANUSCRIPT ACCEPTED SEPTEMBER 25, 2006

MANUSCRIPT HANDLED BY MICHAEL TOPLIS